Sensors and Actuators A 248 (2016) 54–61

Contents lists available at ScienceDirect

Sensors and Actuators A: Physical

journal homepage: www.elsevier.com/locate/sna

Mechanoelectrical transduction in the hydrogel-based biomimetic sensors

F.A. Blyakhman[a,b,*], A.P. Safronov[c], A.Yu. Zubarev[d], T.F. Shklyar[a,b], O.A. Dinislamova[a], M.T. Lopez-Lopez[e]

[a] Department of Biomedical Physics and Engineering, Ural State Medical University, 3 Repin Str., Yekaterinburg 620028, Russian Federation
[b] Department of Physics, Ural Federal University Named After the First President of Russia B.N.Yeltsyn, Yekaterinburg 620083, Russian Federation
[c] Department of Chemistry, Ural Federal University Named After the First President of Russia B.N.Yeltsyn, Yekaterinburg 620083, Russian Federation
[d] Department of Mathematics, Ural Federal University Named After the First President of Russia B.N.Yeltsyn, Yekaterinburg 620083, Russian Federation
[e] Departamento de Fisica Aplicada, Universidad de Granada, 18071 Granada, Spain

ARTICLE INFO

Article history:
Received 29 January 2016
Received in revised form 14 June 2016
Accepted 14 June 2016
Available online 22 July 2016

Keywords:
Biomimetic sensors
Polyelectrolyte hydrogel
Electrical potential
Mechanical deformation
Depolarization
Modeling

ABSTRACT

The study addresses the phenomenon of mechanoelectrical transduction in polyelectrolyte hydrogels and, in particular, the search of the driving force for the change of the electrical potential of a gel under the applied mechanical stretch. Polyelectrolyte gels of calcium and magnesium salts of polymethacrylic acid were synthesized by the radical polymerization in water solution. Their electrical potential measured by microcapillary electrodes was negative and fall within 100–140 mV range depending on the nature of a counterion and the networking density of a gel. The rectangular samples (~10 mm in length and 2 × 2 mm in cross-section) of gel-based sensors underwent the dynamic axial deformation, and the simultaneous monitoring of their geometrical dimensions and the electrical potential was performed. Sensor elongation resulted in the overall increase of gel volume, and it was always accompanied by the gel potential change toward the depolarization (diminishing of the negative values). Theoretical model based on the assumption of the total electrical charge conservation in the course of the dynamic deformation of a filament was proposed to describe the dependence of the electrical potential of a gel on its volume. Good agreement between the predictions of the model and the experimental trend was shown. The proposed mechanism of mechanoelectrical transduction based on the stretch-dependant volume changes in polyelectrolyte hydrogels might be useful to understand the nature of mechanical sensing in much more complex biological gels like the cell cytoskeleton.

1. Introduction

Synthetic polymeric hydrogels are widely introduced as biomimetic materials for the biomedical applications. From the general viewpoint of physical chemistry, the cell, especially its cytoskeleton, structurally resembles a polyelectrolyte hydrogel. Such gel is a 3D cross-linked polymeric network with the electric charges localized on the macromolecular filaments, and with free counterions dispersed in the liquid phase inside the network [1]. The physical basis of the volume contraction and the expansion of polyelectrolyte hydrogels lies in the balance between interaction of polymeric filaments with the medium, the entropic flexibility of filaments, the positive osmotic pressure of counterions, and the balance of attraction and repulsion forces between the electrical charges [2].

Of course, the chemical structure and the mechanisms of molecular interactions in protein network structures in a living cell are much complex than that in synthetic hydrogels. Meanwhile, the close similarity between these two physical systems concerning their structural properties and their response to some basic external stimuli had been demonstrated in numerous studies [3–5] including some performed by us [6–8] earlier.

In particular, both cells and anionic gels are negatively charged in respect to their surroundings, and they both keep electrical potential close to −100 mV. The negative electrical potential of anionic polyelectrolyte gel is a direct result of Donnan equilibrium established on the gel/supernatant boundary [5,6,9,10]. According to IUPAC nomenclature [11], Donnan equilibrium takes place if one

* Corresponding author at: Biomedical Physics Department, Ural State Medical University, 3 Repin Str Yekaterinburg 620028, Russian Federation.
E-mail addresses: Feliks.Blyakhman@urfu.ru, fablyakhman@gmail.com (F.A. Blyakhman).

http://dx.doi.org/10.1016/j.sna.2016.06.020
0924-4247/

or more ionic species for some particular reason cannot cross the phase boundary while other ionic species can freely move across it.

One of the most striking and important phenomena in the cell is the mechanoelectrical transduction (MET). In general, it combines the influence of the mechanical deformation of living cells on their electrical potential [12,13]. The most clear manifestation of MET is the functioning of the excitable cells, especially the muscle cells. In particular, in the cardiomyocytes, where cyclic deformation takes place, MET plays extremely important role in the maintenance of the heart rate pattern [14].

Meanwhile, recently we have demonstrated the existence of MET in synthetic polyelectrolyte gels of calcium and magnesium salts of polyacrylic acid [15,16]. We have shown that the deformation of a gel filament in an axial direction results in the decrease of the negative electrical potential of a gel. We suppose that one of the most reasonable physical mechanisms, which can explain this phenomenon, is the possibility of gel volume changes during the deformation. As the gel is immersed in water, the condition of its constant volume is not applicable as water molecules can enter and exit the interior of gel. Consequently, the gel network extra swelling or contraction may result in the counterions concentration changes of polymer matrix, that may affect the gel electrical potential. Indirectly, the results of theoretical [17,18] and experimental [7] studies that demonstrated the effects of polyelectrolyte hydrogel free swelling on its electrical potential may support the proposed hypothesis.

The objective of the present study was to reveal the correlation between the stretching deformation, the volume changes, and the electrical potential of gel-based sensors. The experimental setup included application of the dynamic axial deformations to the sensors with simultaneous monitoring of their linear dimensions, volume and the electrical potential. Based on the experimental data obtained, we intended to develop a theoretical model for the MET phenomenon in the synthetic hydrogel filament in the ionic solution, which hopefully might be applicable to the wide range of gel systems.

2. Experimental part

2.1. Materials

Polyelectrolyte gels based on poly(methacrylic) acid (PMA) with calcium and magnesium counterions (CaPMA and MgPMA) were synthesized by free-radical polymerization in 2.7 M aqueous solution. Monomer – methacrylic acid and a cross-linker – *N,N'*-methylene-diacrylamide were purchased from (Merck, Schuchardt, Honenbrunn). Polymerization was carried out in polyethylene probe tubes, 10 mm in diameter, at 80 °C for 2 h using ammonium persulfate (APS) as initiator. Prior to polymerization, the monomeric methacrylic acid was completely neutralized by the addition of stoichiometric amount of magnesium or calcium oxides. Cross-linker concentration was set at 1:50, 1:100, 1:200, 1:400 to monomer concentration in molar ratio, which further on is named as the network density of the gel. Subsequent gels are further denoted as Ca(Mg)PMAn, where n stands for the number of monomer units per one cross-link.

After the synthesis, the gels were washed in daily renewed distilled water for two weeks to remove non-reacted monomers, salts, and linear olygomers. The actual content of ionized groups in gels was determined by means of the thermogravimetry (Netzsch STA409 thermal analyzer) by measuring the residual weight after heating of previously dried gels up to 800 °C at a heat rate 10 K/min in the air. During the heating, the gels were decomposed to water, carbon dioxide and the residue of metal oxide. The stoichiometric equation of decomposition gave metal content in the synthesized gel. The content of ionized carboxylate groups was 98% (mol) in CaPMA gels and 75% in MgPMA gels. The synthesis of polymers and their swelling behavior are described in our early publications in details [6,7]. The central part of gel cylinders was cut by a razor blade to elongated rectangular samples, 10 mm in length and approximately 2 × 2 mm in cross-section.

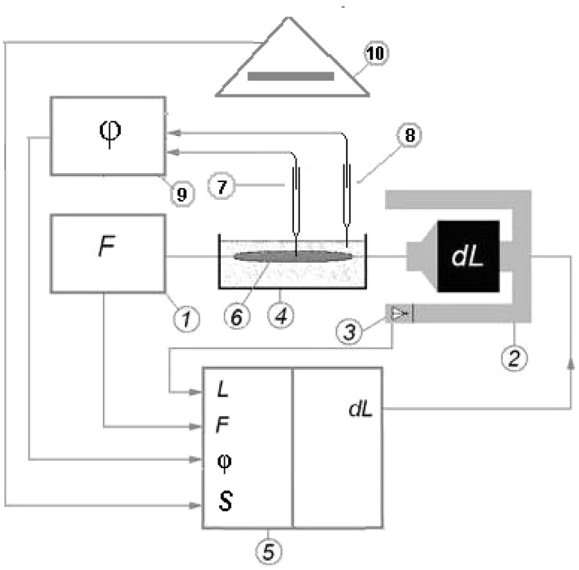

Fig. 1. Scheme of the experimental setup. 1–force transducer, 2 – electromagnetic motor, 3–length transducer, 4–experimental bath, 5–computer, 6–gel sample, 7,8 – glass-micropipette electrodes, 9 – instrumental amplifier, 10 – digital video camera.

2.2. Experimental equipment

Fig. 1 schematically displays the experimental setup of laboratory design used in this study. The equipment was built around an optical system, and contained a thermostatic bath for the gel sample, a semiconductor force transducer, an electromagnetic motor providing mechanical deformations, a semiconductor optical transducer measuring the motor's lever displacement, a personal computer equipped for controlling the experiment.

The electrical potential of a gel sensor was obtained by two identical Ag/AgCl tapered glass microelectrodes (~1 μm in tip diameter) typically used in biophysical studies for intracellular voltage measurement. The details of Donnan potential measurement in the gel were described in several studies [3,4,7]. Briefly, thin-walled, single-barrel borosilicate capillary tubes "TW150F-6" ("World Precision Instruments", USA) were single-pulled using a standard electrode puller "ME-3" ("EMIB Ltd", Russia). The pulled electrodes were immersed in a 3 M KCl solution with the tip facing upward, so that the solution climbed to the tip by capillary action.

One electrode was pinned into the gel sample, the other was placed in water outside. The potential difference between microelectrodes was measured using an instrumental amplifier on the base of an integrated circuit "INA 129" ("Burr-Brown", USA). The main amplifier parameters were: input impedance – 10^{10} Ω, frequency bandwidth – 0...107 Hz, gain – 50. To reduce the influence of electromagnetic interference on the potential difference measurement, special wire shields were provided around the unit. Typically, the peak-to-peak noise at the output of instrumental amplifier during the gel potential monitoring was no higher of 5 mV.

Computerized optical system on the base of digital video camera ("Panasonic" HX-WA2) was used for the monitoring of gel sensor

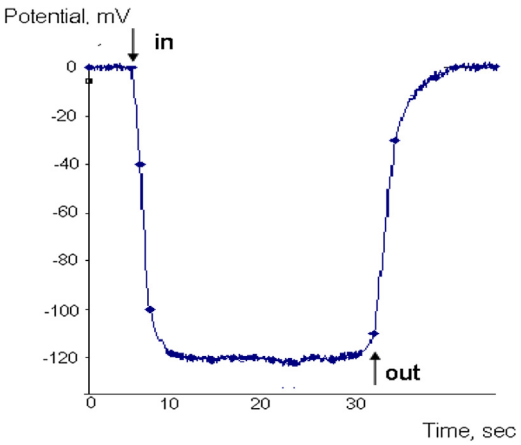

Fig. 2. Typical experimental plot of potential measurement on the MgPMA50 gel sensor.

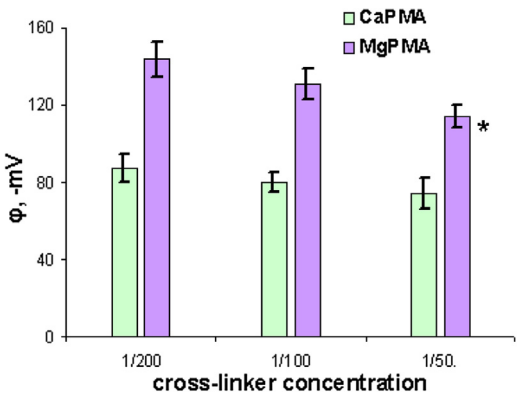

Fig. 3. Potential of CaPMA and MgPMA hydrogels in non-deformed state. Cross-linker concentration presented as the number of the monomer units per one cross-link. Error bars mark standard deviation of the potential mean value (n = 6). Asterisk demonstrates the significant difference between MgPMA50 and MgPMA100 with $P < 0.05$; MgPMA50 and MgPMA200 samples with $P < 0.01$.

planar projection. The camera was placed beneath of the bath's transparent bottom, and video files were recorded.

2.3. Experimental protocol

All experiments were performed at room temperature on gels immersed in distilled water. One end of a rectangular gel sensor ~10 mm in length and ~2 mm in width was affixed to the force transducer or stationary lever, while the other end was connected to the linear motor. The linear motor provided the stepwise or oscillatory triangular axial linear deformations of the gel sensor (see Fig. 1). The generator of signals under the original software controlled the performance of linear motor. In the stepwise regime, the electrical (Donnan) potential (φ) of the gel sensor was measured after each deformation step as the sensor length was kept constant. If oscillatory triangular deformations with the rate from $0.4^{*}10^{-4}$ to $1.6^{*}10^{-4}$ meter per second were applied, the dynamics of the deformation, the planar projection and the potential of the gel were recorded simultaneously in a ~1.0 s interval. The value of the deformation (ε) was determined as the length of the stretched filament related to its initial length:. $\varepsilon = Li/Lo$ The planar projection was recorded optically and then outlined by hand using the original software to determine the current volume of the filament.

2.4. Statistical analysis

The statistic software package StatSoft was used for the statistical analysis. Mean and standard deviation (SD) of the measured parameters were calculated. To estimate the interrelation between measured values, the correlation tests and the regression analysis were performed.

3. Results

Fig. 2 shows the typical experimental plot of the electrical potential (φ) measurement in a polyelectrolyte MgPMA50 gel by a capillary microelectrode. The baseline with $\varphi = 0$ corresponds to allocation of electrode in a supernatant solution outside the gel sample. Upon pinning the capillary electrode into the gel, its potential dropped down to the value ca. −120 mV, which remained constant. When the electrode was taken out, φ returned to the baseline.

The negative electrical potential of anionic polyelectrolyte gel is a result of the difference in the concentration of counterions inside and outside the gel. The concentration of $[Mg^{2+}]$ counterions inside the negatively charged gel network is higher than that in the surrounding water medium. In general, it means that such a difference arise from an electrical driving force that accounts for the Donnan potential [6,10].

Fig. 3 shows the dependence of the gel potential on the nature of divalent counterions (Ca^{++}, Mg^{++}) and on the gel network density. The negative values the Donnan potential of MgPMA gels are twice higher than that of CaPMA gels. It means that the polymeric network of MgPMA gels is electrically charged to a higher extent than CaPMA network. Most likely, it indicates that Ca^{2+} cations form stronger bonds with carboxylate residues of PMA network than Mg^{2+} cations. Hence, free counterion concentration inside CaPMA gel is lower and its negative electrical potential is lower too.

In addition, Fig. 3 demonstrates a distinct diminishing trend in the potential with the increase of the network density in the both series of gels. In case of CaPMA the difference between the mean values of the potential for gels with different network density is not substantial, but in the case of MgPMA50 hydrogels it is statistically distinguished. The close correlation between the potential and the network density for the both series of gels was found: correlation coefficients were 0.98 for CaPMA and 0.97 for MgPMA. Obtained result implies that the lower is the gel network density the higher is the value of the negative potential of Ca(Mg)PMA gel. This conclusion is in an accord with the results obtained earlier [16].

The periodical mechanical deformation applied to the gel sensor changed its potential. Fig. 4 shows the time course of triangular linear axial deformation applied to the gel sample and the corresponding gel potential measured simultaneously. During the stretch of a sample, initial negative value of the gel potential shifted toward the depolarization. It means that the gel became less negatively charged. During the release phase of the deformation, the restoration of gel potential took place. The depolarization – restoration cycles closely followed the stretch – release cycles.

Table 1 presents the result of gel potential measurements obtained in MgPMA200 sensors in the course of step-wise deformation. Mean values (n = 7) and SD of potential at different extent of sample stretch are presented. One can see that the elongation of

Table 1
Dependence of the gel sensor (MgPMA200) potential on the applied stretch.

Deformation, Li/Lo	Potential, mV
1,00	−123 ± 4
1,05	−119 ± 5
1,10	−113 ± 3
1,15	−104 ± 6
1,20	−100 ± 3

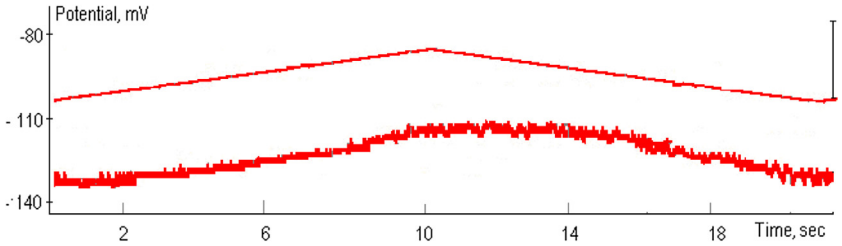

Fig. 4. Typical experimental record of the MgPMA100 gel potential under applied cyclic deformation. Upper curve corresponds to the output of optical transducer, which measured the motor lever displacement. Lower curve is the output of instrumental amplifier, which measured the gel sensor potential simultaneously. The scale bar on the right corresponds to 1.0 mm of the sample elongation.

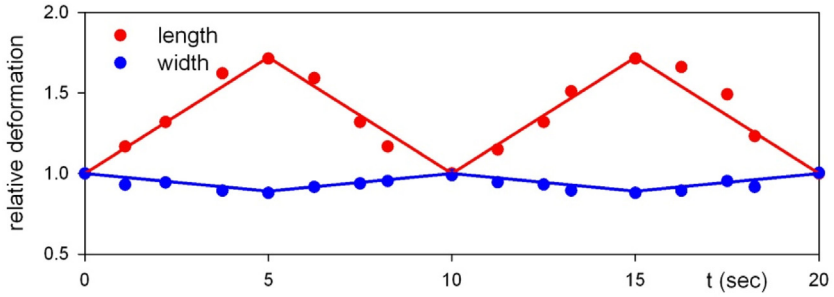

Fig. 5. Dynamics of the gel sensor (MgPMA200) length and width under the applied triangular linear axial deformations.

the gel sensors resulted in the decrease of negative values of the potential. Close inverse correlation between the gel potential and the gel stretch was found (r = – 0.99).

The length and the width of the gel filament were monitored during the deformation cycles, and Fig. 5 shows the time dependence of their values related to the non-deformed state. At the phase of the applied stretch in 5 s, the length of sensor increased 1.7 times, while the relative width decreased only to 0.9. At the phase of sample release, its length decreased and the width increased back. It is evident from Fig. 5 that the increase in relative length of the sensor is much larger than the decrease in its width. It means that the volume of filament does not keep constant during deformation cycles.

The estimation of the filament volume as the product of its length and square of the width revealed that the volume increased at the stage of stretch application and decreased at the release stage. Fig. 6 presents the generalized dependence of the relative volume changes of the gel filament upon its relative elongation due to the applied stretch. Mean values and SD of relative volume change at the maximum of applied stretch for several CaPMA and MgPMA gel-based sensors are plotted.

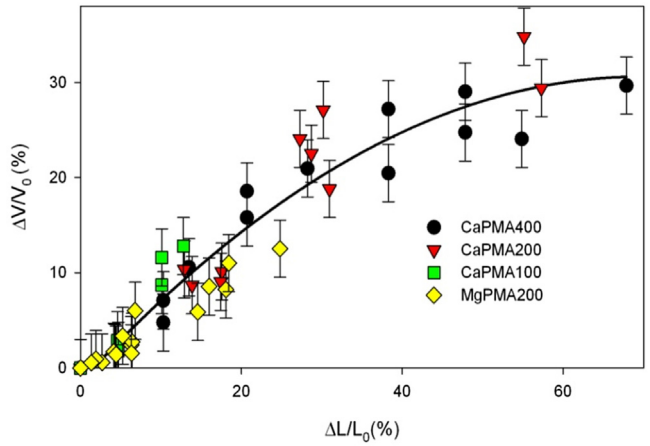

Fig. 6. Dependence of sensor volume changes under stretch.

It is clear that the volume of the gel filament does not stay constant if elongating deformation is applied. The dependence appeared to be rather universal in the series of gels studied in the present work. Within the experimental error, the relative volume changes for MgPMA and CaPMA gels with different network density fit the same curve up to 25% stretch of samples. It shows a close to linear increase, and tends to saturation at higher elongations of CaPMA gel sensors with network density of 1:200 and 1:400. The volume increase is rather substantial: it is more than 10% at a 20% stretch.

It looks reasonable that such induced swelling of a gel upon its deformation can provide the consequent changes in its electrical potential. To disclose the possible interrelation between these factors we introduce the following theoretical model.

3.1. Model

Theoretical determination of the electrical potential inside the rectangular prism-shaped samples requires cumbersome calculations and the final results can not be presented in a compact analytical form. That is why for the maximal simplification of mathematics, we will consider a cylindrical polymeric gel filament with the length L which is much larger than its radius R. The filament is placed in an infinitive liquid with the dielectric permeability ε. The cylindrical model of the sample allows us to get the final results in mathematically and physically transparent form and keeps all physically principal points of the experimental situation.

In our experiments, the monovalent negative ions COO^- are fixed on the polyelectrolyte chains which constitute the gel network; movable counterions Mg^{++} are distributed inside and outside the filament. Let us denote the total negative electrical charge, the gel chains carry on, as $-Q$.

The supernatant liquid outside the filament contains Mg^{++} counterions, which form a double electrical layer around the filament. Besides, the aqueous supernatant contains H^+ and OH^- ions originated from the self dissociation of water molecules. At the infinite

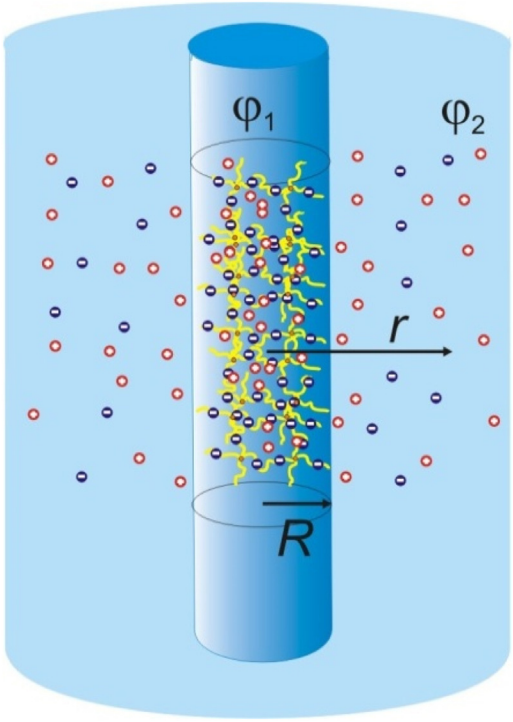

Fig. 7. Sketch of the model under consideration.

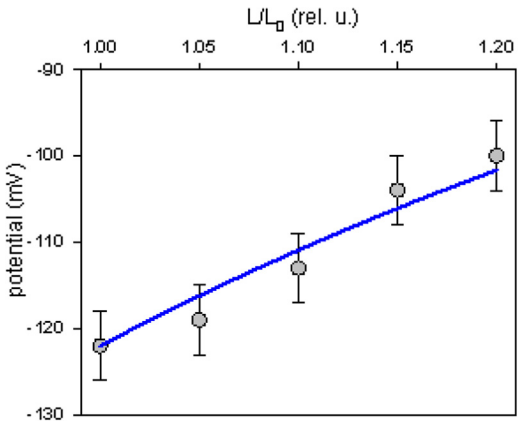

Fig. 8. Dependence of the potential of MgPMA200 gel on the applied stretch. Line corresponds to the fitting of experimental points by the model Eq. (8).

distance from the filament, the electroneutrality condition is maintained.

It is evident from Fig. 5 that the width of filament slightly decreases if the filament is stretched. However, the decrease is very small and for the sake of simplicity we took the radius of the model filament being constant during deformation. Note, that Fig. 6 demonstrates almost linear increase of the sample volume with it's elongation, at least till 40 per cent of the relative stretch. This means that within the framework of these deformations, change of the filament width with it's elongation is negligible and can be ignored. It should be noted that the condition of the permanent width of the sample is not crucial for the model and can be easily modified to incorporate the slight decrease of the width at increase of the filament length.

Our aim is to find the mean, over the filament cross-section, magnitude <φ> of the electrical potential inside the filament as a function of its length. The considered model is illustrated in Fig. 7.

Let us denote $\rho_c = \frac{Q}{\pi R^2 L}$ the absolute magnitude of the mean density of the charges, adsorbed on the filament chains; $\rho_1(r)$ is the total charge density the inside the filament; the local charge density outside the fiber we will denote as $\rho_2(r)$. Here r is a distance from the cylinder axis (see Fig. 7).

The electrical potentials φ_1 and φ_2 inside and outside the filament respectively, satisfy the Poisson equations

$$\nabla^2\varphi_1 = -\frac{4\pi}{\varepsilon}\rho_1, r < R \tag{1}$$

and

$$\nabla^2\varphi_2 = -\frac{4\pi}{\varepsilon}\rho_2, r > R \tag{2}$$

Inside the filament, the electrical charge consists of the negative charge directly situated on the polymer chains as well as on the charges of the motile positive and negative ions. We will suppose that the total charge Q of the ions fixed on the chains is not changed during the elongation of the filament. This assumption is justified by the high energy of the ions adsorption on the chains.

In contrast, the charge, provided by the motile ions, can alternate due to the change of the condition of thermodynamic equilibrium between the ions inside and outside the filament. Here it is worth noting that the total charge of the polyelectrolyte filament with all the counterions should be zero to obey the electroneutrality condition. However, this condition is not strictly fulfilled in the layers adherent to the surface of the filament as counterions are free to move to the supernatant. Therefore, these layers carry on non-compensated negative charge. Usually, the law of the fixed ions spatial distribution inside the polymer filament is unknown. We suppose, for simplicity, that this distribution is homogeneous, i.e. it does not depend on r. This assumption corresponds to the fact that the filament is optically transparent and is supported by the comparison of the theoretical and experimental results (see Fig. 8). That means that this is structurally homogeneous. The motile ions inside and outside the filament obey the Boltzmann law of distribution.

Taking it into account in the Debye – Huckel approximation $q_{\pm}\varphi_{1,2} \ll kT$, by using (2), we get the following equation for the potential outside the filament:

$$\nabla^2\varphi_2 = \kappa^2\varphi_2 \tag{3}$$

Here $\kappa = \sqrt{\frac{4\pi}{\varepsilon kT}\left(q_+^2 n_+ + q_-^2 n_-\right)}$ is the inverse Debye thickness of the double electrical layer, n± and $q_{\pm}$ are the concentrations of the positive and negative ions infinitely far from the filament and their charges respectively. One can show easily that in the framework of the Debye – Huckel approximation the charge density of the motile ions is significantly less than that of the charges fixed on the chains and can be neglected. In the framework of this approximation, the charge density inside the filament coincides with the uniform density of the fixed charges ρ_c.

Taking it into account we get the following solutions of the Eqs. (1) and (3):

$$\varphi_1 = \frac{\pi}{\varepsilon}\rho_c r^2 + A$$

$$\varphi_2 = BH_0(kr) \tag{4}$$

here $H_0(x)$ is the modified Hankel function, A and B are constants to be determined.

Their magnitudes can be found from the following standard boundary relations of electrostatics:

$$r = R, \varphi_1 = \varphi_2, \frac{\partial\varphi_1}{\partial r} = \frac{\partial\varphi_2}{\partial r} \tag{5}$$

The fact that the carrier liquid (water) takes place not only outside, but also inside the filament is taken into account here. Therefore, the dielectric permeability inside the sample, in the first

approximation, coincides with the permeability of the surrounding medium. That is why we use the simplification that the dielectric permeability ε inside and outside the polymer filament is the same.

Combining Eqs. (4) and (5) we get:

$$\varphi_1(r) = \frac{\pi}{\varepsilon}\rho_c\left[r^2 - R^2 + 2\frac{RH}{\kappa H'}\right]$$
$$H = H_0(\kappa R),\ H' = \frac{dH_0(x)}{dx}|_{x=\kappa R} \quad (6)$$

The average, over the fiber cross-section, electrical potential is:

$$\langle\varphi_1\rangle = \frac{2}{R^2}\int_0^R \varphi_1(r)\,dr = -\frac{\pi}{\varepsilon}\rho_c\left(\frac{1}{2}R^2 - 2\frac{RH}{\kappa H'}\right) \quad (7)$$

Let us note that the Hankel function, being positive, monotonously decreases, therefore the inequality $H'<0$ is held. Thus, the relation in the square brackets of (7) is positive.

For the majority of the typical situations the strong inequality $\kappa R \gg 1$ is fulfilled. By using the well-known asymptotic expressions for the Hankel function, in this limiting case we have:

$$\mathrm{H} = \frac{\exp(-\kappa R)}{\sqrt{\kappa R}},\ H' = -\frac{1}{2}\frac{\exp(-\kappa R)}{(\kappa R)^{3/2}}(1+2\kappa R) \approx -H$$

By using this estimate in (7), one can get

$$<\varphi_1> = -\frac{\pi}{\varepsilon}\rho_c\left[\frac{1}{2}R^2 - 2\frac{R}{\kappa}\right] \approx -\frac{\pi}{2\varepsilon}\rho_c R^2 \quad (8)$$

Let ρ_{c0} be that charge density inside the fiber when its length is L_0. Since the total charge $-Q$ of the filament is permanent, the following relation

$$\rho_1(L) = \rho_{c0}\frac{L_0}{L} \quad (9)$$

is held. By using (9) in Eqs. (7) or (8), one can see, that absolute magnitude of the negative average potential $<\varphi_1>$ decreases while the fiber length L increases. This conclusion, at least qualitatively, corresponds to the trend of diminishing of the magnitude of gel potential observed in experiment.

The quantitative agreement is surprisingly also good. As we do not have actual data on the magnitude of Q, we have estimated the value $\frac{\pi}{2\varepsilon}\rho_{c0}R^2$ from the condition that the estimate (8) fits the experimental results for $L = L_0$.

Fig. 8 shows the calculated dependence of the potential on the stretch of gel filament given by solid line in comparison with the experimental data presented in Table 1. It is seen that the model curve nicely fits experimental points.

4. Discussion

This work addressed the electrical and mechanical properties of polyelectrolyte hydrogels based on poly(methacrylic) acids. The effects of many factors, such as the degree of gel swelling, the composition and the ionic strength of the surrounding solution, the type of counterions, the gel network density on the gel potential and gel elasticity were defined and reported in a series of our publications [6–8,16]. Besides, we demonstrated that at a given deformation velocity, the extent of gel deformation closely correlates with the gel potential. Furthermore, we found that at the same level of gel deformation, the lower is the deformation velocity, the higher is the relative change of gel electrical potential [15].

As a result of these earlier studies, CaPMA and MgPMA gels with the network density of 1:200–1:400 were chosen as most suitable prototypes of the gel mechanoelectrical sensor with the sensitivity of 1–2 mV per 1% of deformation depended on the network density and the regime of stretching [19]. According to mechanical examination of these gels used [8,16], the stress of 30–50 N/m^2 resulted in 1% of gel sample stretching deformation.

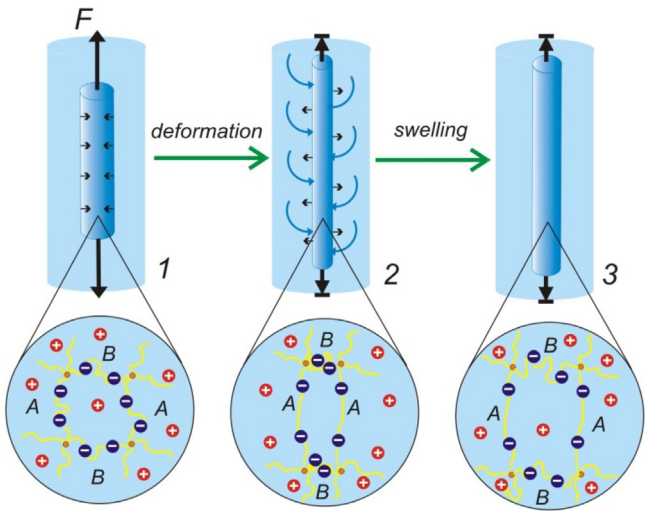

Fig. 9. Scheme of gel swelling induced by its deformation. Upper row – macroscopic forces and fluxes. Lower row – microscopic view on polymer network. 1–initial structure of gel, 2–gel structure under strain; volume remains constant, 3–gel structure under strain; volume increased due to the swelling. *A* – polymeric subchains oriented along the direction of elongation. *B* – polymeric subchains oriented across the direction of elongation.

The main point of present investigation is a search for a reasonable mechanism to explain the MET in hydrogels-based sensors. Possible impact of gel stretch-dependant volume change on the gel potential was our working hypothesis. To test this, the advanced experiments with simultaneous measurements of the gel volume and gel potential in the course of applied stretching deformation were performed, and the theoretical model based on these results was developed. Given the good correlation between the model predictions and the actual mechanoelectrical transduction in polyelectrolyte filament, we may turn to the possible physical reasons, which underlie the electrical response of the synthetic hydrogel to the mechanical stimuli.

The ability of polymeric network to swell in a liquid under the applied stretching deformation was one of the first theoretical results of the classic Flory theory of polymer solutions experimentally confirmed for some swollen rubber materials [20,21]. In general, a polymeric network tends to swell in the plane across the direction of stretching. The basic reason is the tendency of a polymeric subchain to keep its equilibrium conformation of a random Gaussian coil. The applied force stretches the coils of subchains along the direction of its action. The subproduct of this stretching is the compression of polymeric coils in a plane across this direction under the normal stresses. As the compression is thermodynamically unfavorable, the random coil tends to reestablish equilibrium dimensions by the absorption of a solvent and swelling. In case of polyelectrolyte network, this general trend is enforced by electrostatic contribution, which is illustrated in Fig. 9. For the sake of simplicity, the process is shown in a step-wise fashion.

Mark 1 in Fig. 9 corresponds to the initial network structure of polyelectrolyte gel, which is to be deformed by the applied stress. Let us define two types of polymeric subchains between the cross-links, which constitute the network. Subchains marked *A* are positioned along the applied force, subchains marked B are oriented across the direction of elongation. The non-deformed network structure is isotropic: both subsets of polymeric subchains are statistically equivalent. Their conformation is close to statistical coil. There are negatively charged residues affixed at the subchains and the equivalent number of positively charged counterions, which compensate the electrical charge of the chains. If elongating stress

is applied, the normal stresses appear at the walls of the sample, and lead to the contraction of the gel across the direction of elongation.

Mark 2 in Fig. 9 shows the result of the elongating deformation if the volume of the gel remained constant. The network structure becomes anisotropic: while subchains *A*, which carry the load, stretch along the direction of deformation, subchains *B* compress due to the applied normal stresses. The compressed compact conformation of subchains *B* is unfavorable both as it deviates from the conformation of a random coil and as the distance between adjacent residues diminishes and the electrostatic repulsion between them increases. To recover the conformation of a statistical coil and to decrease the electrostatic repulsion in subchains *B* gel absorbs water from the supernatant and swells. Mark 3 in Fig. 9 shows that due to the swelling of gel across the direction of elongation subchains *B* uncurl and the distance between negatively charged residues allocated on them increases.

The increase of the gel volume due to its swelling results in the diminishing of the total charge density of the polymeric network. Effectively, the network becomes less charged. It seems reasonable to conclude that the negative potential of gel will also diminish; i.e. the gel will depolarize. The model developed above rigorously confirms this intuitively clear inference.

Meanwhile, there are certain limitations in both the experimental setup and the theoretical modeling. For instance, we have supposed that such processes as the dissociation of polar groups in the network, the condensation of counterions, and the ionic equilibrium at the surface are not affected by the stretching deformation. It might be true at a short time scale but the condition of static ionic distribution in the stretched gel will certainly be violated in long time intervals. Good correlation between the values of the potential measured and calculated in the model show that at the characteristic time scale of the dynamic stretching, which was around 5 s for each consequent phase, ionic distribution in the gel filament apparently stayed constant.

Based on these considerations one would then expect the reverse polarization of the permanently stretched gel in a long time interval due to the slow relaxation to the equilibrium ionic distribution.

5. Conclusions

By the consistent measurements of the geometrical dimensions and the electrical potential of the gel sensor under the dynamic periodical stretching deformation, we have found that the filament swells at the elongating step and deswells at the release step. Simultaneously, the negative values of gel potential diminish if gel filament swells due to its stretching and increase at gel contraction. The dependence of the potential upon gel volume is adequately described by a theoretical model based on the assumption of the total electrical charge constancy of the gel filament in the course of dynamic deformation. The quantitative agreement between experimental and calculated values of the potential is achieved. These results clarify the underlying physical principle of the mechano-electrical transduction in gel-based devices, which may be widely introduced as the biomimetic sensors of strain, stress, and stretch.

Acknowledgments

This work has been done under the financial support of the Russian Scientific Fund, project 14-19-00989. One of us (M.T. Lopez-Lopez) has been supported by the Grant FIS2013-41821-R (MINECO, Spain).

References

[1] R.S. Harland, R.K. Prudhomme, Polyelectrolyte Gels: Properties, Preparation and Applications, American Chemical Society, Washington DC, 1992.
[2] S. Hirotsu, in: K. Dusek (Ed.), Responsive Gels: Volume Transitions II, Advances in Polymer Sciences, Springer-Verlag, Berlin, 1993, p. 275.
[3] G.N. Ling, Revolution in the Physiology of the Living Cell, Krieger Pub, Co., Malabar, 1992.
[4] G.H. Pollack, Cells Gels and the Engines of Life, Ebner&Sons, Seattle, 2001.
[5] R.W. Guelch, J. Holdenried, A. Weible, T. Wallmersperger, B. Kroeplin, Electroactive polymer actuators and devices, Proc. SPIE 3987 (2000) 193–202.
[6] A.P. Safronov, T.F. Shklyar, V. Borodin, Y.A. Smirnova, S.Yu. Sokolov, G.H. Pollack, F.A. Blyakhman, in: G. Pollack, I. Cameron, D. Wheatley (Eds.), Donnan Potential in Hydrogels of Poly(Methacrylic Acid) and Its Potassium Salt, Water in Biology, Springer, 2006, pp. 273–284.
[7] T.F. Shklyar, A.P. Safronov, I.S. Klyuzhin, G.H. Pollack, F.A. Blyakhman, A correlation between mechanical and electrical properties of the synthetic hydrogel chosen as an experimental model of cytoskeleton, Biophysics 53 (2008) 544–549.
[8] T.F. Shklyar, A.P. Safronov, O.A. Toropova, G.H. Pollack, F.A. Blyakhman, Mechanical characteristics of synthetic polyelectrolyte gel as a physical model of the cytoskeleton, Biophysics 56 (2011) 68–73.
[9] F. Gao, F.B. Reitz, G.H. Pollack, Potentials in anionic polyelectrolyte hydrogels, J. Appl. Polym. Sci. 89 (2003) 1319–1321.
[10] H. Guo, T. Kurokawa, M. Takahata, W. Hong, Y. Katsuyama, F. Luo, J. Ahmed, T. Nakajima, T. Nonoyama, J. Gong, Quantitative observation of electric potential distribution of brittle polyelectrolyte hydrogels using microelectrode technique, Macromol. Articles ASAP (2016), http://dx.doi.org/10.1021/acs.macromol.6b00037.
[11] IUPAC Compendium of Chemical Terminology, 1997.
[12] O.P. Hamill, B. Martinac, Molecular basis of mechanotransduction in living cells, Physiol. Rev. 81 (2001) 685–6740.
[13] P.G. Gillespie, R.G. Walker, Molecular basis of mechanosensory transduction, Nature 413 (2001) 194–202.
[14] T.A. Quinn, P. Kohl, U. Ravens, Cardiac mechano-electric coupling research: fifty years of progress and scientific innovation, Prog. Biophys. Mol. Biol. 115 (2014) 71–75.
[15] T.F. Shklyar, A.P. Safronov, O.A. Toropova, G.H. Pollack, F.A. Blyakhman, Mechanoelectric potentials in synthetic hydrogels: possible relation to cytoskeleton, Biophysics 55 (2010) 931–936.
[16] T.F. Shklyar, O.A. Dinislamova, A.P. Safronov, F.A. Blyakhman, Effect of cytoskeletal elastic properties on the mechanoelectrical transduction in excitable cells, J. Biomech. 45 (2012) 1444–1449.
[17] L. Feng, Y. Jia, X. Chen, X. Li, L. An, A multiphasic model for the volume change of polyelectrolyte hydrogels, J. Chem. Phys. 133 (2010) 114904.
[18] L. Feng, Y. Jia, X. Li, L. An, Comparison of the multiphasic model and the transport model for the swelling and deformation of polyelectrolyte hydrogels, J. Mech. Behav. Biomed. 4 (2011) 1328–1335.
[19] F. Blyakhman, A. Safronov, T. Shklyar, Biomimetic sensors of the mechanoelectrical transduction based on the polyelectrolyte gels, Key Eng. Mater. 644 (2015) 4–7.
[20] P.J. Flory, J. Rehner, Statistical mechanics of cross-linked polymer networks II swelling, J. Chem. Phys. 11 (1943) 521–526.
[21] L.R.G. Treloar, The swelling of cross-linked amorphous polymers under strain, Trans. Faraday Soc. 46 (1950) 783–789.

Biographies

Prof. Felix A. Blyakhman, graduated Urals State University (Yekaterinburg, Russia) in 1979 (Biology), got Ph.D. in 1986 (Physiology) and D.Sc. in 1996 (Transplantology and artificial organs) at Moscow's Institute of Transplantology and Artificial Organs. Present employment: Head of Biomedical physics and Engineering Dept., Ural State Medical University (Yekaterinburg); Prof. of Physics Dept., Ural Federal University (Yekaterinburg). Current field of interest: muscle physiology, biological motility, biomedical physics and engineering, biomimetics.

Prof. Alexander P. Safronov, graduated Urals State University (Yekaterinburg, Russia) in 1982 (Chemistry), got Ph.D. in 1989 (Physical Chemistry) and D.Sc. in 2000 (Thermodynamics and Molecular Physics) at Urals State Technical University (Yekaterinburg, Russia). Present employment: Prof. of Chemistry Dept., Urals Federal University (Yekaterinburg). Current field of interest: polymer physical chemistry, thermodynamics, blends and composites, aqueous polymer solutions and gels, biomimetics.

Prof. Andrey Yu. Zubarev, graduated Urals State University (Yekaterinburg, Russia) in 1979 (Physics), got Ph.D. in 1986 and D.Sc. in 1993 (Physical Chemistry) at Urals State University (Yekaterinburg, Russia). Present employment: Prof. of Mathematical Dept., Urals Federal University (Yekaterinburg). Current field of interest: physics of polymers, colloids and fluids, mathematical modeling of these systems.

Dr. Tatyana F. Shklyar, graduated Urals State University (Yekaterinburg, Russia) in 1979 (Biology), got Ph.D. in 1988 (Pharmacology) and D.Sc. in 2012 (Physiology) at South Urals Pedagogical University (Chelyabinsk). Present employment: Leading Researcher of Biomedical physics and engineering Dept., Urals State Medical University (Yekaterinburg); Prof. of Physics Dept., Urals Federal University (Yekaterinburg). Current field of interest: muscle physiology, polyelectrolyte gel properties, biomimetics.

Olga A. Dinislamova, graduated Urals State University (Yekaterinburg, Russia) in 2008 (Physics) and got M.S. (Medical Physics). Present employment: Researcher of Biomedical physics and engineering Dept., Urals State Medical University (Yekaterinburg). Current field of interest: polyelectrolyte gel properties.

Dr. Modesto T. Lopez-Lopez, got B.Sc. in Physical Sciences, University of Granada, Spain (2001), Ph.D. in Physics, University of Granada, Spain (2005). Present employment: Associate Professor at the Department of Applied Physics of the University of Granada (Spain). Current field of interest: Experimental study of magnetic fluids, suspensions and polymer systems.